

MORPHOLOGY AND MICROSTRUCTURE PROPERTIES OF NANOZEOLITE COATING ON IRON FOAM WITH VARIATION OF CALCINATION TEMPERATURE AND CHITOSAN

Vinda Puspasari

Research Center for Metallurgy and
Materials
Indonesian Institute of Sciences
vind001@lipi.go.id

Permana Andi Paristiawan

Research Center for Metallurgy and
Materials
Indonesian Institute of Sciences

Satrio Herbirowo

Research Center for Metallurgy and
Materials
Indonesian Institute of Sciences

Bintang Adjiantoro

Research Center for Metallurgy and
Materials
Indonesian Institute of Sciences

Porous materials are widely used in various applications such as ion exchange, separation, drug delivery sensor and water filter application. However porous iron is susceptible to corrosion, therefore coating with corrosion resistant materials is requirede.g. with nanozeolite material. For the application as filter, nanozeolite improves the activities characteristic of iron foam surface since it can act as the agent of ion exchangers and absorb heavy metal ions in water. In the present study, porous metal was coated with nanozeolite by sol-gel coating method. Chitosan concentrations and calcination temperatures are the variable parameter to be optimized in the present research. The mass change of the sample decreases as the chitosan addition increases. The mass change also decreases as the calcination temperature increases. The highest mass change occurs for sample 1 at 14.63%. The morphology of nanozeolite layer showed that the addition of chitosan can decrease the agglomeration of nanozeolite coating. The higher of calcination temperature can homogenize the nanozeolite layer. The particle form of nanozeolite through SEM revealed needle-like, rod and spherical shape. The addition of chitosan can decrease the cluster of nanozeolite particle and the higher of calcination temperature make them more uniform after calcination process. The XRD characterization of sample 5 showed that the nanozeolite particle in this sample was amorphous.

Keywords: Nanozeolite, Iron Foam, Chitosan, Morphology, Microstructure Properties, SEM-EDS, XRD Characterization.

1. INTRODUCTION

The present, porous materials are widely used in many potential application such as catalyst, filtration, ion exchange, drug delivery, sensors, and as electrode materials in batteries [1]. Porous materials are divided into microporous (pores size are smaller than 2 nm), mesoporous (pores size are larger than 50 nm) [2]. Porous inorganic materials also have many superiority as ion exchange materials and catalysis application such as the removal of toxic heavy metals from waste stream, water softening, and radioactive waste control [3]. Metal foam is one example of porous inorganic materials which is made from many various elements such as aluminum, iron, titanium, tantalum and many others [4]. The characteristics of metal foam are have light mass, high porosities, good energy compression and energy absorption and good strength properties [5]. In this research, we use ferrous metal foam as based materials. The scientist have been reported that iron foam as an efficient method for removing organic

pollutant such as dyes from water [6].

Iron foam with open pores can function as a filter which can be used for water filter applications. Iron foam can act as a filter because it has tight and open and very small size pores so that it can filter out particles that are larger than the pore and trap impurities on the pore walls [7]. The optimization of filtration function in ferrous metal foam can be increased using materials which have high adsorption properties such as activated carbon, silica gel, graphite and zeolite [8]. Activated carbon is less economically as an adsorbent than zeolites because of the high cost of regeneration system [9]. The zeolite is chosen because of its low-cost and more economically. Zeolite doesn't require a complicated regeneration system, so it doesn't require high disposal costs after use [10]. Besides that, zeolite also have good corrosion resistance properties which can increase corrosion properties of metal foam [11]. As we know that metal foam is easily to corrode because of its reaction with corrosive environment. Zeolites can be alternative materials from chromate because of its environmental friendly properties [12]. Zeolites are one kind of minerals which contain aluminosilicate ranging from colorless to white or light res because of the existence of impurities and minerals traces [13]. The important properties of zeolites are as selective absorber, ion exchanger, and high catalytic properties. Recent research interest has focused on synthesis nano-crystalline zeolite because of their better properties for adsorption processes [14]. There are some aspect which affect the affectivity of nano zeolite such a concentration of surfactant, working temperature, contact time and pH of the solution [10].

In this research, nano zeolite was made using sol gel method to be coated on iron foam. Nano zeolite coating was made on iron foam to construct the walls of mesoporous materials which can be effective for membrane support in water filtration process [15]. Chitosan is used as a template for self-assembly monolayer in nano zeolite coating [16]. In addition, chitosan is also known as a material which have good inhibitor corrosion properties [17]. Sol-gel coating is chosen in this experiment because of its promising excellence, such as superior adhesion, good barrier properties, and high chemical and thermal stability. The variation of calcination temperature can affect Nano zeolite coating on iron foam was made in three steps, they are the preparation of chitosan solution, preparation of Na-Al-Si sol gel solution, and zeolite coating on iron foam. This paper also study the effect of calcination temperature and concentration of chitosan to the mass change, chemical elements, morphology, and microstructure properties of nano zeolite. The characterization for nano zeolite coated on iron foam are mass change, XRD (X-Ray Diffraction), SEM (Scanning Electron Microscope) and EDS (Energy Dispersive Spectroscopy).

2. METHOD

2.1 Materials and Equipment

Materials used in this experiment are iron foam (cell size = 580 μm ; area density = 450g/m²; thickness = 1.9 mm) dimensi 1x1 cm, aqua demineralizers, sodium hydroxide, aluminum nitrate anhydrate, sodium silicate, acetic acid, chitosan. Equipment used in this experiment are hot plate, oven, SEM-EDS, XRD.

2.2 The Preparation of Chitosan Solution

The methods of this research employed and is began with preparation of 1% and 2% (wt/vol) chitosan solution and preparation of Na-Al-Si sol-gel solution. Na-Al-Si sol-gel solution is coated on iron foam using sol-gel dip coating. The 1% of chitosan solution is made from 1 gram of chitosan powder which is mixed using 2 mL acetic acid and 98 mL demineralized. The solution mixture then stirred for 12 hours until dissolved. The same procedure also used for 2% chitosan solution.

Figure 1 shows 1% and 2% of chitosan solution which have been made.



Figure 1: The 1% and 2% chitosan solution

2.3 The Preparation of Na-Al-Si Solution

The Na-Al-Si sol-gel solution is made by prepare a 0.4 M $\text{Al}(\text{OH})_3$ solution by dissolving 3 grams of NaOH in 15 mL of demineralizer aqua and 3.75 grams of $\text{Al}(\text{NO}_3)_3 \cdot 9\text{H}_2\text{O}$ added gradually until dissolved. After that, demineralizer aqua is added until the volume of the solution reaches 25 mL. Then, the pH of the solution was measured with pH meter paper and the resulting pH was 13. The second solution prepared is 0.6 M $\text{Si}(\text{OH})_3$ solution by dissolving 2.6 mL of Na_2SiO_3 with a concentration of 5.7 M in 22.4 mL of demineralizer aqua. The $\text{Si}(\text{OH})_4$ solution is made in a plastic glass so that the silica element in the beaker does not contaminate the sodium silicate solution. The two solutions are then mixed and obtained a Na-Al-Si sol-gel solution which can be seen in Figure 2.



Figure 2: The Na-Al-Si sol-gel solution

2.4. Sol-Gel Dip Coating

Sol-gel coating was conducted by preparing Na-Al-Si sol gel solution and 1% and 2% chitosan solution. Iron foam is dipped in the chitosan solution for 1 minute as can be seen in **Error! Reference source not found.**. After that, the sample is placed in a petri dish and heated at 100°C for 5 minutes. After that, the iron foam is dipped in the sol gel solution for 1 minute as seen in Figure 4, then heated in the oven at 100°C for 1 minute. These steps are carried out once again. After coating process is complete, the iron foam is placed in a combustion boat as shown in

Figure 5, then the calcination process is carried out in a nitrogen furnace with variation temperature of 300°C , 400°C , and 500°C for two hours. The variation of calcination temperature is chosen because the calcination temperature below 700°C can maximize the surface area, porosity, and homogeneity of nanozeolite [18].

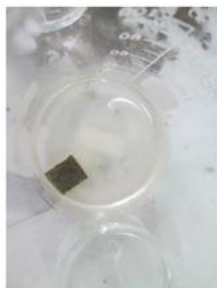


Figure 3: Dipping process of iron foam in chitosan solution

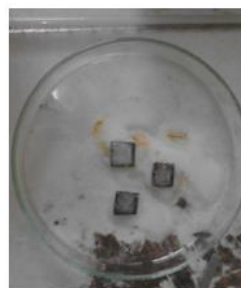


Figure 4: Result of Na-Al-Si sol-gel coating



Figure 5: Laying of nanozeolite coated porous iron on combustion boat

The iron foam which have been coated by nanozeolite is ready to be characterized by mass change characterization, SEM, EDS, and XRD. The name of the samples in Table 1 are based on the variation of chitosan content and calcination temperature.

Table 1: Variation of Chitosan Addition and Calcination Temperature

Sample Code	%Chitosan	Calcination Temperature (°C)
1	1%	300
2	1%	400
3	1%	500
4	2%	300
5	2%	400
6	2%	500

3. RESULTS AND DISCUSSION

3.1 The Mass Change

Before coating process on the iron foam samples, the initial and final mass of iron foam was measured to know that the coated layer is formed. Table 2 and Figure 6 show the mass change which occurred after the coating and calcination processes. The mass change of the sample decrease as the chitosan addition increase. The mass change also decrease as the calcination temperature increase. The decrease of mass change is caused by the release of gases, such as CO₂ that occur in the temperature range of 500°C and degradation of chitosan which is burned at a temperature of 500°C which has about 50% of the remaining mass [19]. The decrease of mass change is also caused by the release of precursor when the calcination temperature increases [20].

Table 2: Mass before and after calcination process

Sample Code	Initial Mass (g)	Final Mass (g)	Mass Change (g)	Mass Change (%)
1	0.041	0.047	0.006	14.63

2	0.040	0.045	0.005	12.50
3	0.036	0.040	0.004	11.11
4	0.057	0.065	0.008	14.04
5	0.056	0.062	0.006	10.71
6	0.053	0.058	0.005	9.43

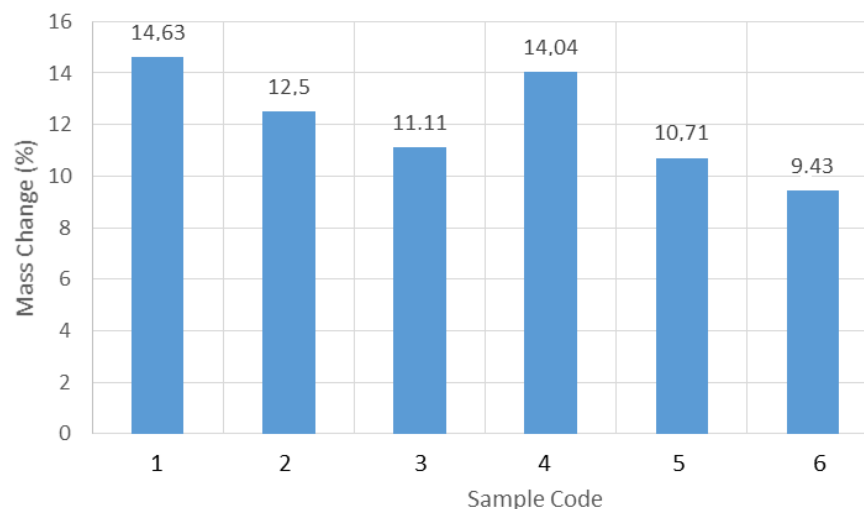


Figure 6: Mass change for all samples

3.2 The Effect of Chitosan Addition and Calcination Temperature to Morphology of Nanozeolite on Iron Foam

The effect of chitosan addition and calcination temperature to morphology of nanozeolite on iron foam is characterized by SEM (scanning electron microscope). The SEM characterization is located on the top of specimen surface. Figure 7 shows the morphology of nanozeolite coating of sample 1. The results of SEM characterization showed that nanozeolite layer form on the surface of sample 1. There is also a nanozeolite layer which fills the pores of iron foam which can decrease the adsorption properties of iron foam. Nanozeolite layer looks agglomerated and not evenly spread homogeny on the surface. The agglomeration is caused by chitosan which has not been completely degraded in calcination temperature of 300°C. The formation of agglomerate in the surface of iron foam can reduce the surface area and decrease the interaction between nanozeolite and iron foam. This phenomenon can decrease the physical properties of material [21]. Figure 8 showed the morphology of nanozeolite coating of sample 2. The results of SEM characterization showed that nanozeolite has formed more homogeny on the sample surface than sample 1 although there are some agglomeration on the sample surface. The particle of nanozeolite is not homogeneously dispersed, resulting the agglomeration of silicate layer in the surface of iron foam matrix [22].

Figure 9 shows the morphology of nanozeolite coating of sample 3 (sample with 1% chitosan addition and 500°C of calcination temperature). The results of SEM characterization showed that nanozeolite layer form on the surface of sample is the most homogeny from all the samples. Moreover, it was also seen that there is less agglomeration occurred in the sample 3. The pores in the sample 3 are more open than sample 1 and 2 because the increase of calcination temperature can evaporate chitosan more than the other samples [9]. The degradation temperature of chitosan is about 500°C resulting the nanozeolite coat perfectly on iron foam. The more open of nanozeolite-iron foam pores can increase surface area and adsorption properties of

nanozeolite-iron foam. Figure 10 showed the morphology of nanozeolite coating of sample 4 (sample with 2% chitosan addition and 300°C of calcination temperature). The chitosan addition can affect the morphology of nanozeolite on iron foam and acted as template in coating process of nanozeolite to iron foam surface [23]. From Figure 9 it can be seen that the addition of chitosan content can decrease agglomeration of nanozeolite. The agglomeration in sample 4 is less than sample 1 which have less of chitosan content. The agglomeration decrease as composition content of chitosan increases.

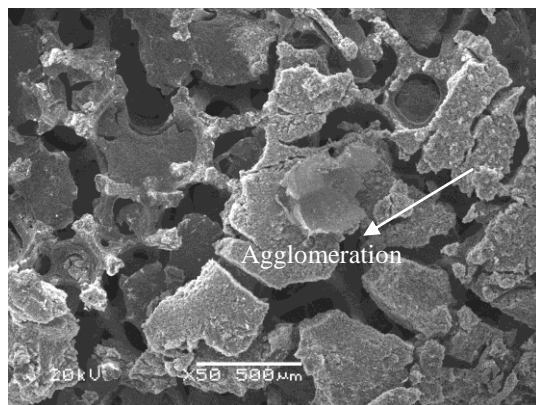


Figure 7: Morphology of nanozeolite coating of sample 1

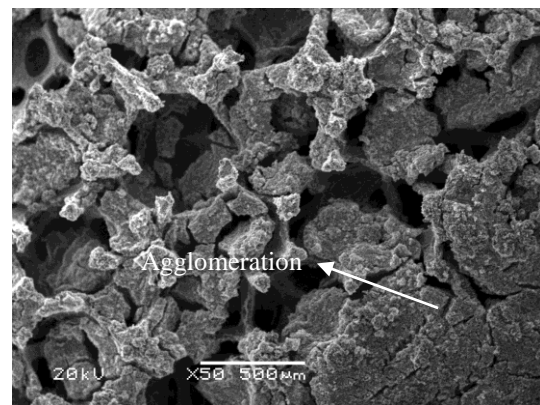


Figure 8: Morphology of nanozeolite coating of sample 2

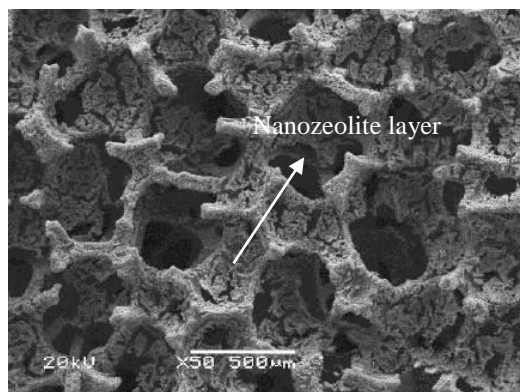


Figure 9: Morphology of nanozeolite coating of sample 3

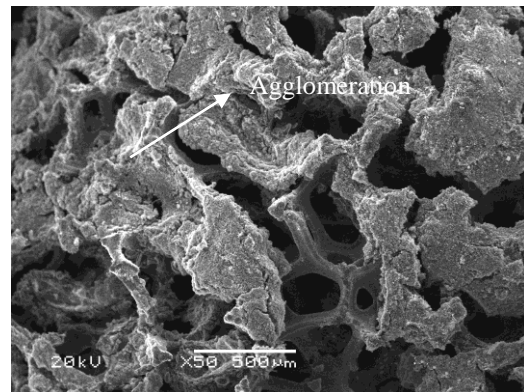


Figure 10: Morphology of nanozeolite coating of sample 4

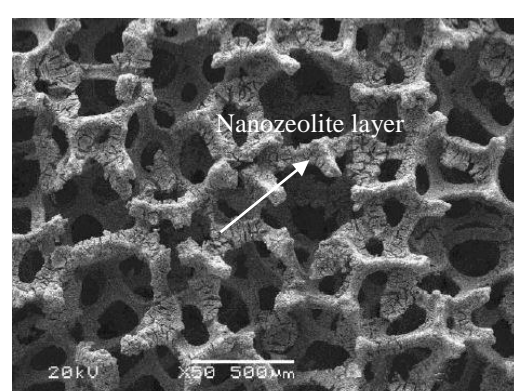
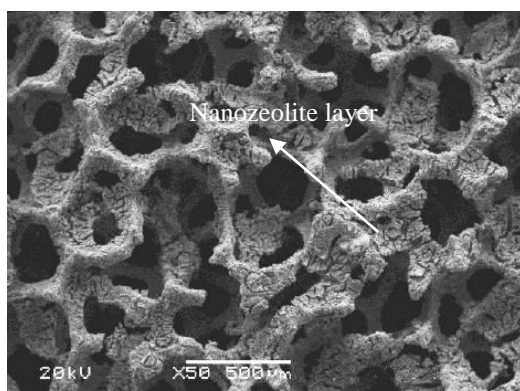


Figure 11: Morphology of nanozeolite coating of sample 5

Figure 12: Morphology of nanozeolite coating of sample 6

Figure 11 shows the morphology of nanozeolite coating of sample 5 (sample with 2% chitosan addition and 400°C calcination temperature). From figure 10 it can be seen that nanozeolite layer which formed on the iron foam surface is more homogeny and less of agglomeration. The chitosan as precursor solution has plenty of hydroxyl and amine groups which helps the nanozeolite particle to stick strongly on the iron foam substrate [24]. The higher chitosan content can increase wetting of nano zeolite particle. The higher of calcination temperature made the zeolite coating denser with minimal intracrystal porosity resulting the more open pores of nanozeolite-iron foam. Figure 12 showed the morphology of nanozeolite coating of sample 6 (sample with 2% chitosan addition and 500°C calcination temperature). The nanozeolite layer which formed in the surface of iron foam follow the pore shape of iron foam. The layer of nanozeolite coating in this sample is denser and not cover the pores than the other samples. The higher calcination temperature of 500°C in this sample make the nanoparticles are more uniform in the surface of iron foam. This phenomenon caused by the process of silica dissolution and crystallization produced more uniform nanoparticles during calcination process [7].

3.3. The Effect of Chitosan Addition and Calcination Temperature to Nanozeolite Particle Form

The effect of chitosan addition and calcination temperature to pericle form and shape of nanozeolite coating on iron foam is characterized by SEM (scanning electron microscope). The SEM characterization is located on the cross section of specimen surface.

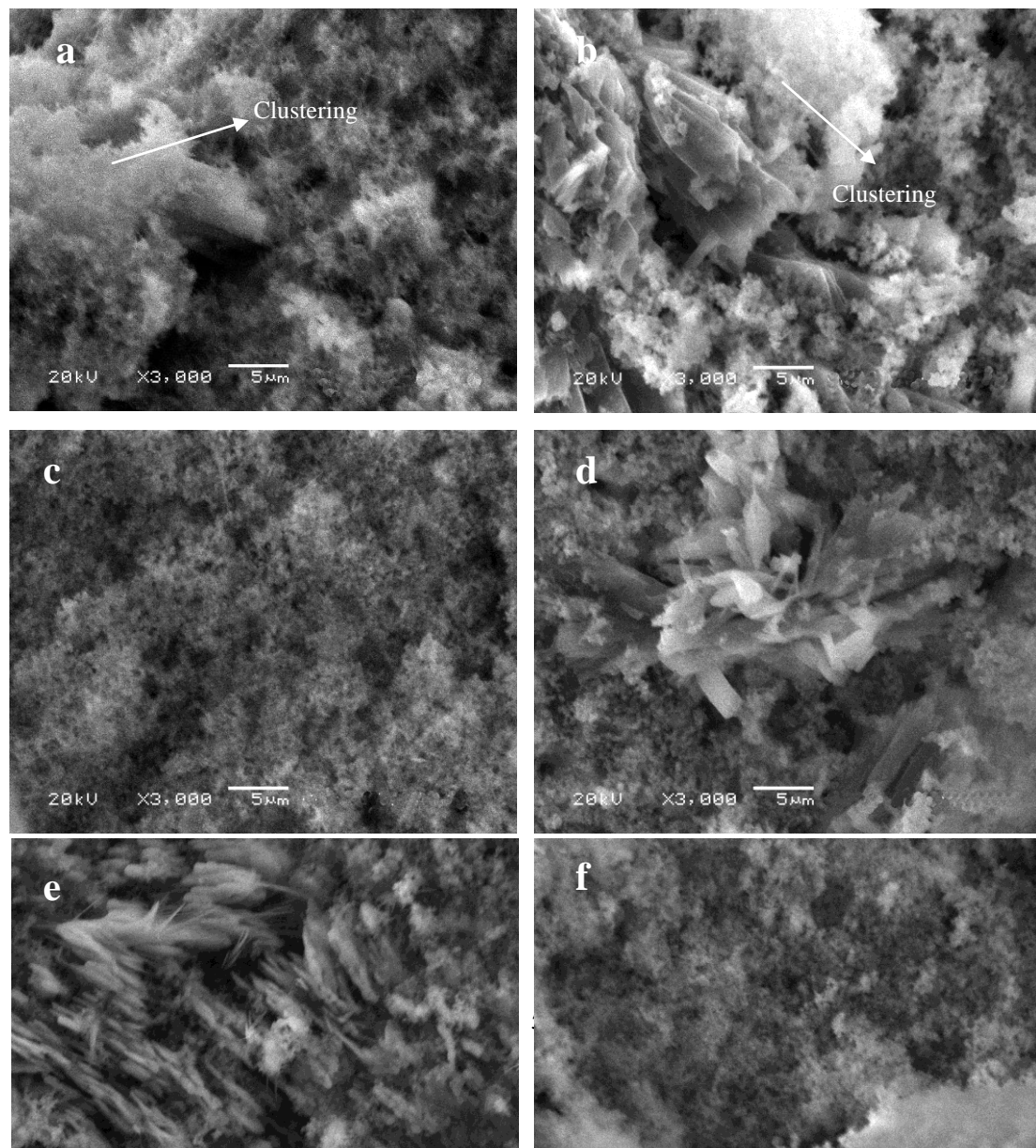


Figure 13: Nanozeolite particle forms of (a) Sample 1, (b) Sample 2, (c) Sample 3, (d) Sample 4, (e) Sample 5, (f) Sample 6

Figure 13 (a) shows the cross section of SEM result of nanozeolite coating of sample 1 (sample with 1% chitosan addition and 300°C calcination temperature). It can be seen that the form of nanozeolite particles are needle-like shaped. According to the picture, it was known that the nanozeolite particles generated clusters. Clustering phenomenon could occur during sol-gel coating continued by calcination process [2]. Figure 13 (b) shows the cross section of SEM result of nanozeolite coating of sample 2 (sample with 1% chitosan addition and 400°C calcination temperature) which shows particle form of nanozeolite. The nanozeolite particle seen as rod-shape and some of them seen as spherical shape. The appearance of nanozeolite particle of sample 2 is almost spherical compared to sample 1. The nanozeolite particles still formed cluster. The EDS result showed that the sample 2 contain Si, Al, Na, and O elements.

Figure 13 (c) shows the cross section of SEM result of nanozeolite coating of sample 3 (sample with 1% chitosan addition and 500°C calcination temperature) which shows particle form of nanozeolite. The nanozeolite particle is more homogeny in this sample. The shape of nanozeolite particle is spherical. Calcination temperature of 500°C is enough temperature to conduct silica dissolution and crystallization process which produced more uniform nanoparticles [3]. Figure 13 (d) shows the cross section of SEM and EDS result of nanozeolite coating of sample 4 (sample with 2% chitosan addition and 300°C calcination temperature) which shows particle form of nanozeolite. The nanozeolite particle of sample 4 showed rod-shape particles in the center of Figure 16 and surrounded by spherical particles. The cluster of particles in this sample decrease because of the addition of chitosan content [2].

Figure 13 (e) shows the cross section of SEM results of nanozeolite coating of sample 5 (sample with 2% chitosan addition and 400°C calcination temperature) which shows particle form of nanozeolite. The nanozeolite particle of sample 5 showed needle-like and spherical particles. Figure 13 (f) showed the cross section of SEM results of nanozeolite coating of sample 6 (sample with 2% chitosan addition and 400°C calcination temperature) which shows particle form of nanozeolite. The increase of calcination temperature conduct silica dissolution and crystallization process which produced more uniform nanoparticles [25].

3.4. The EDS Results of Nanozeolite Particle

The EDS results show the %mass of elements which are contained in the sample.

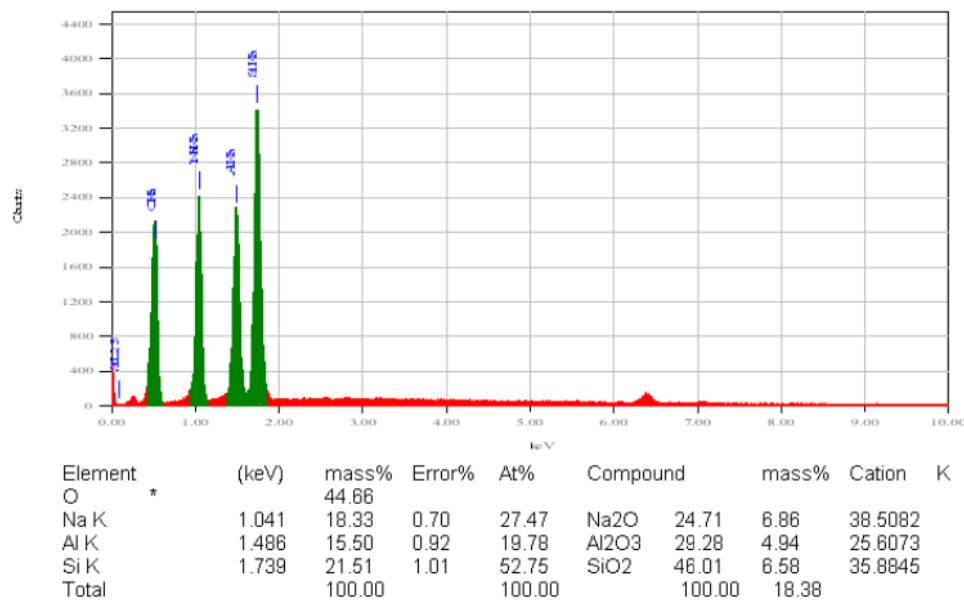


Figure 14 shows the EDS result of sample 1 which contain of 18.33 %mass of Na, 15.50 %mass of Al, 21.51 %mass of Si, and 44.66 %mass of O elements. The EDS result proved that nanozeolite was formed on the surface layer of iron foam. Figure 15 shows the EDS result of sample 4 which contain of 20.29 %mass of Na, 14.33 %mass of Al, 21.30 %mass of Si, and 44.08 %mass of O elements. The EDS result proved that nanozeolite was formed on the surface layer of iron foam. The EDS results of all samples were summarized in Table 3.

Table 3 shows the EDS results of %atom of nanozeolite. All the samples contain Na, Si, Al, and O elements and the highest content of Al and Si elements is sample 5 (sample with 2% chitosan addition and 300°C calcination temperature). The lowest content of Si and Al elements is sample 6 (sample with 2% chitosan addition and 500°C calcination temperature). As shown in Table 3, the ratio of Si:Al in sample with 1% chitosan addition is lower than sample with 2% of chitosan addition. This phenomenon caused by the higher content of chitosan increase amine and hydroxyl functional group which can bind more Si and Al elements [12]. The ratio of Si:Al in each sample is different but the value tends to be close to each other. The average value of Si:Al in all sample is 1,41. The ratio of Si:Al in all samples showed value between 1-1,5 which close to Zeolite-X value, so it can be concluded that the zeolite formed in this experiment is Zeolite-X [26]. Figure 16 shows the XRD characterization of nanozeolite in sample 5. According to the XRD analysis, the nano zeolite particle was amorphous. This amorphous form of nano zeolite is an advantage in the preparation of silicon-based materials, because the silica is tend to be active in its amorphous form [27].

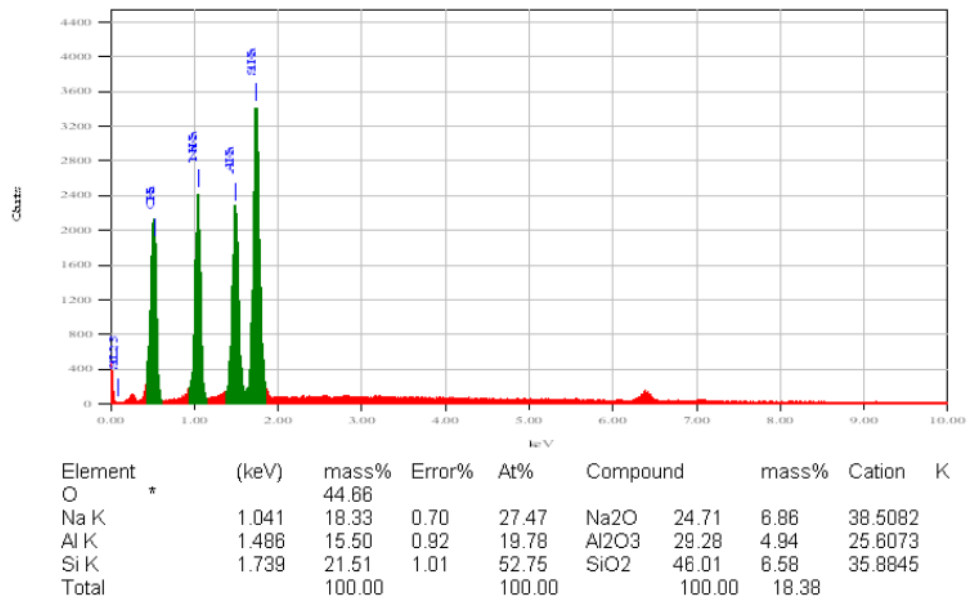


Figure 14: EDS result of sample 1

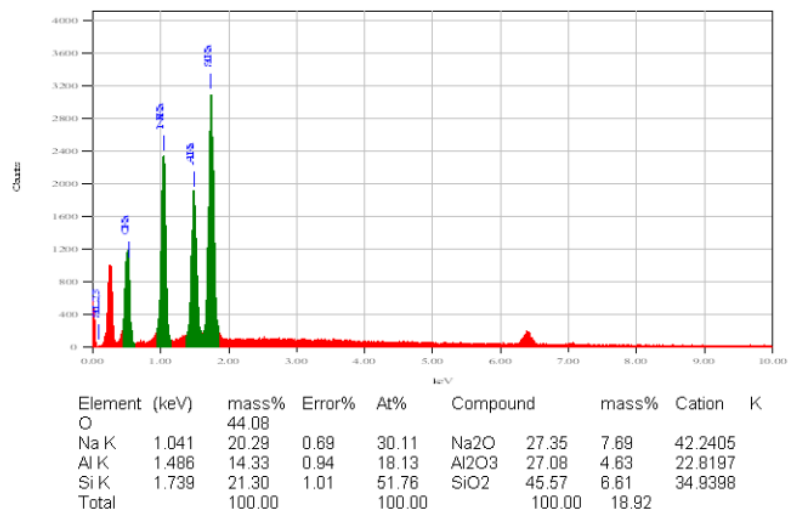


Figure 15: EDS result of sample 4

Table 3: EDS results of nanozeolite

Sample	%At Na	%At Si	%At Al	%At O	Si:Al
1	19.98	22.85	16.07	41.10	1.42
2	25.63	19.88	14.16	40.33	1.4
3	19.46	22.89	16.25	41.40	1.4
4	24.13	26.93	17.23	31.70	1.56
5	18.31	23.81	17.00	40.89	1.4
6	32.94	13.22	10.03	43.81	1.31

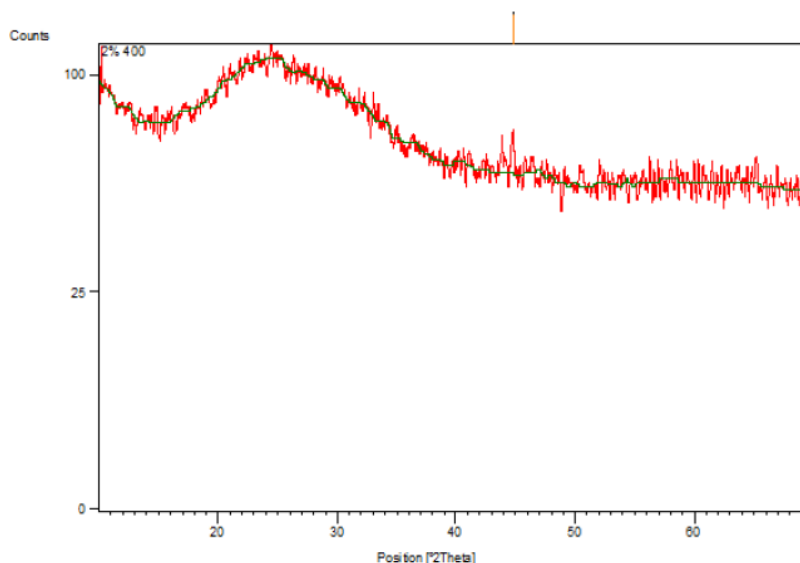


Figure 16: XRD characterization of nanozeolite in sample 5

4. CONCLUSION

This research had nanozeolite coating on iron foam in this experiment. The nanozeolite coated on iron foam was characterized by mass change measurement, SEM-EDS, and XRD. The mass change of the sample decrease as the chitosan addition increase. The mass change also decrease as the calcination temperature increase. The highest mass change is sample 1 of 14.63%. The morphology of nanozeolite layer result showed that the addition of chitosan can decrease agglomeration of nanozeolite coating. The higher of calcination temperature can homogenize the nanozeolite layer. The particle form of nanozeolite through SEM revealed needle-like, rod, spherical shape of nanozeolite particles. The addition of chitosan can decrease the cluster of nanozeolite particle and the higher of calcination temperature make them more uniform after calcination process. The XRD characterization of sample 5 showed that the nanozeolite particle in this sample was amorphous.

5. REFERENCES

- [1] AKHTAR, F., ANDERSSON, L., OGUNWUMI, S., HEDIN, N., BERGSTROM, L., "Structuring adsorbents and catalysts by processing of porous powders", *Journal of The European Ceramic Society*, v. 34, n. 7, pp. 1643-1666, 2014.
- [2] COOPER, A. I., "Porous molecular solids and liquids", *ACS Central Science*, v. 3, n. 6, pp. 544-553, 2017.
- [3] POHL, A., "Removal of heavy metal ions from water and wastewaters by sulfur-containing precipitation agents", *Water, Air, & Soil Pollution*, v. 231, n. 503, 2020.
- [4] GARCIA-MORENO, F., "Commercial applications of metal foams: Their properties and production", *Materials*, v. 9, n. 2, pp. 20-24, 2016.
- [5] Lee, C., Lee, S., Park, J. et al., "Removal of copper, nickel and chromium mixtures from metal plating wastewater by adsorption with modified carbon foam", *Chemosphere*, v. 166, pp. 203-211, 2017.
- [6] HUANG, Y., LUO, M., XU, Z., ZHANG, D., LI, L., "Catalytic ozonation of organic contaminants in petrochemical wastewater with iron-nickel foam as catalyst", *Separation and Purification Technology*, v. 211, pp. 269-278, 2019.
- [7] HUANG, Y., JIANG, J., MA, L. et al., "Iron foam combined ozonation for enhanced treatment of pharmaceutical wastewater", *Environmental Research*, v. 183, Jan, 2020.
- [8] AMELIA, S., MARYUDI, M., "Application of natural zeolite in methylene blue wastewater treatment process by adsorption method," *Jurnal Bahan Alam Terbarukan*, v. 8, n. 2, pp. 144-147, 2019,
- [9] PHAM, T. H., LEE, B. K., KIM, J., "Improved adsorption properties of a nano zeolite adsorbent toward toxic nitrophenols," *Process Safety and Environmental Protection*, v. 104, pp. 314-322, 2016

- [10] TRI, N., THANG, P., TAN, L., Removal of phenolic compounds from wastewaters by using synthesized Fe-nano zeolite,” *Journal of Water Process Engineering*, v. 33, pp. 101070, 2020.
- [11] AL-SUBAIE, M., AL-TURKUSTANI, A., SELVIN, R. et al., “anticorrosion nanocrystalline beta zeolite thin film for advanced applications”, *Journal of Chemistry*, pp. 693730, 2015
- [12] YANG, H., LI, W., LIU, X. et al., “Preparation of corrosion inhibitor loaded zeolites and corrosion resistance of carbon steel in simulated concrete pore solution,” *Construction and Building Materials*, v. 225, pp. 90–98, 2019.
- [13] ANIS, S., SINGARAVEL, G., HASHAIKEH, R., “Electropsun Ni-W/zeolite composite fibers for n-heptane hydrocracking and hydroisomerization”, *Materials Chemistry and Physics*, v. 200, pp. 146–154, 2017.
- [14] HUONG, P., LEE, B., KIM, J., “Improved removal of 2-chlorophenol by a synthesized Cu-nano zeolite”, *Process Safety and Environmental Protection*, v. 100, pp. 272–280, 2016.
- [15] JIMENEZ-CASTANEDA, M., MEDINA, D., “Use of surfactant-modified zeolites and clays for the removal of heavy metals from water”, *Water (Switzerland)*, v. 9, n. 4, 2017.
- [16] DE HARO-DEL RIO, D. A., RIZVI, S., MCGLACKEN, M. et al., “Synthesis of nanozeolites/carbon composites for the adsorption of bivalent copper”, *Journal of Water Chemistry and Technology*, v. 40, n. 5, pp. 272–278, 2018.
- [17] HIDAYATULLAH, S., GAPSARO, F., SETYARINI, P. H., “Pengaruh variasi korosi inhibitor dari kitosan sisik ikan terhadap perilaku korosi besi astm a36: studi ekstrapolasi tafel dan eis”, *Rekayasa Mesin*, v. 11, n. 1, pp. 51-59, 2020.
- [18] MENAD, K., FEDDAG, A., RUBENIS, K., “Synthesis and study of calcination temperature influence on the change of structural properties of the LTA zeolite”, *Rasayan Journal of Chemistry*, v. 9, n. 4, pp. 788-797, 2016.
- [19] WOLSKA, J., SETKOWICZ, J., MALISZEWSKA, I. H., “Preparation and characterization of chitosan-agar films”, *Progress on Chemistry and Application of Chitin and its Derivatives*, v. 25, pp. 210-226, 2020.
- [20] MIRBALOOCHZEHI, M. R., REZVANI, A., SAMIMI, A., SHAYESTEH, M., “Application of a novel surfactant-modified natural nano-zeolite for removal of heavy metals from drinking water”, *Advanced Journal of Chemistry A*, v. 2020, n. 5, pp. 612–620, 2020.
- [21] CALABRESE, L., “Anticorrosion behavior of zeolite coatings obtained by in situ crystallization: A critical review,” *Materials*, v. 12, n. 1, 2018.
- [22] GULTOM, F., AGUNG, U. D., “Pengaruh penambahan nanozeolit alam dalam preparasi nanokomposit foam poliuretan terhadap sifat mekanik,” *Jurnal Darma Agung*, v. 17, n. 3, pp. 1179–1190, 2019
- [23] WULANDARI, I. O., MARDILA, V. T., SANTJOJO, D. J., SABARUDIN, A., “Preparation and characterization of chitosan-coated Fe_3O_4 nanoparticles using ex-situ co-precipitation method and tripolyphosphate/sulphate as dual crosslinkers,” In: *IOP Conference Series: Materials Science and Engineering*, v. 299, n. 1, pp. 0–8, 2018.
- [24] CALLISTER, W. D., RETHWISCH, D. G., *Fundamental of materials science and engineering: an integrated approach*, 4 Ed., New York, John Wiley & Sons, Inc, 2012.
- [25] EL HANACHE, L., SUNDERMANN, L., LEBEAU, B., “Surfactant-modified MFI-type nanozeolites: Super-adsorbents for nitrate removal from contaminated water”, *Microporous and Mesoporous Materials*, v. 283, pp. 1–13, 2019.
- [26] KIHARA, T., ZHANG, Y., HU, Y., MAO, Q., TANG, Y., MIYAKE, J., “Effect of composition, morphology and size of nanozeolite on its in vitro cytotoxicity”, *Journal of Bioscience and Bioengineering*, v. 111, n. 6, pp. 725–730, 2011.
- [27] GHASEMI, Z., YOUNESI, H., KAZEMIAN, H., “Synthesis of nanozeolite sodalite from rice husk ash without organoc additives”, *The Canadian Journal of Chemical Engineering*, v. 89, n. 3, pp. 601-608, June, 2011.